TABLE IV. Ground-state g values of rhombic spectra.

	Optical results						ESR results[a]				
Wavelength of zero-field line	$H\|\|[100]$ g_1	g_2	$H\|\|[111]$ g_3	g_4	g_5	ESR Center	$H\|\|[100]$ g_1	g_2	$H\|\|[111]$ g_3	g_4	g_5
9736.6 Å	1.467	4.974	1.240	5.843	5.603	R_1	1.408	4.996	1.208	5.967	5.538
9764.7 Å	3.383	4.670	2.137	7.079	3.578	R_2	3.329	4.650	2.075	7.168	3.556
						R_3	1.333	2.502	1.180	2.591	3.094
						R_4	2.175	4.711	1.852	5.414	5.414

[a] Calculated from Ref. 1.

D. Rhombic Spectra

The lines at 9736.6 Å and 9764.7 Å have been examined along [100] and [111] directions. The spectra were more complex than those described above, and the overlapping of lines sometimes gave rise to ambiguous interpretations for one particular pattern. However, only one self consistent set of g values resulted when both orientations were taken into account. In Table IV the ground-state g values predicted from ESR for these directions are compared with those observed. The overlapping of lines gave rise to an error which we have not been able to estimate so that no errors are included in the optical g values reported for the rhombic spectra. However, it is clear that the shorter wavelength line is R_1 and the other line R_2. Thus, we have removed the ambiguity left in the earlier investigation and are able to report the excited-state g values. We have computed the principal g values and these are presented in Table III. The g values observed in our chosen directions are rather insensitive to the values of g_y and g_z, and in consequence the values of these two parameters which give a least-squares fit carry a larger uncertainty.

6. CONCLUSIONS

We have confirmed all but one of the correlations reported by Kirton and McLaughlan and have removed the ambiguity about the lines belonging to the rhombic ESR spectra R_1 and R_2. We have shown with 90% confidence that the upper-state splitting of Yb^{3+} in cubic sites is greater than 18.3 cm^{-1}. Excited-state g values have been tabulated for the identified sites.

PHYSICAL REVIEW VOLUME 178, NUMBER 2 10 FEBRUARY 1969

Anomalous Population Distributions in an Optically Excited Metastable Level in $CaF_2:Tm^{2+}$

C. H. ANDERSON AND E. S. SABISKY
RCA Laboratories, Princeton, New Jersey 08540

(Received 3 October 1968)

The population distribution among the magnetic sublevels of the metastable state of $CaF_2:Tm^{2+}$ is shown to be strongly influenced by spin orientation memory from the ground state. This memory is dependent on the wavelength and polarization of the pump radiation, being quite strong at 5790 Å. The population is also influenced by an optical cross-relaxation or excitation transfer between neighboring ions, particularly so because the hyperfine splittings in the ground and excited states are almost identical. Also, it is shown that there is a high degree of nuclear spin orientation memory.

I. INTRODUCTION

THIS is the second of two papers on paramagnetic resonance in the optically excited metastable level in $CaF_2:Tm^{2+}$. The first paper[1] dealt with the measurement of the g value and hyperfine constants in the excited state and the comparison of these values with crystal-field theory. This paper is concerned with the anomalous population distributions observed in the magnetic sublevels in the excited state and their interpretation.

A normal Boltzmann distribution among the magnetic sublevels of an optically excited state will be observed if the spin lattice relaxation rate between the sublevels is fast compared to the optical decay rate out of the state. However, if the normal thermalization rate is slower than the decay rate, the population distribution in the magnetic sublevels can become sensitive to other processes, which can result in very different distributions. Under the latter condition in $CaF_2:Tm^{2+}$, we have observed two distinct mechanisms which are important in determining the population distribution. The first is what we call spin orientation memory, which

---

[1] E. S. Sabisky and C. H. Anderson, Phys. Rev. 148, 194 (1966).

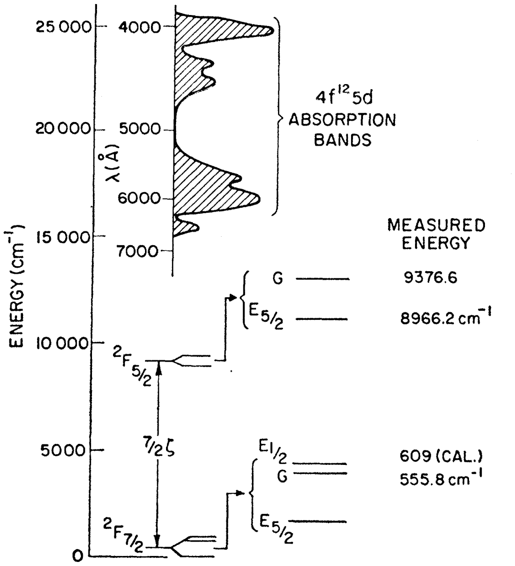

FIG. 1. Energy levels of CaF_2:Tm^{2+}.

occurs when the angular momentum in the excited state has a preference to lie along the same axis that it had in the ground state before the optical excitation. This memory would normally not be expected to occur in a solid when the excitation is into a broad absorption band which is then followed by a series of nonradiative decays before reaching the metastable level. However, it appears to be a general phenomenon, since similar effects have been observed in a defect center in CaO [2] and in ruby.[3,4] We also have evidence that there is a high degree of spin orientation memory for the Tm^{169} nuclear spin through the optical pump cycle. The second population-determining mechanism is an optical cross-relaxation process that is closely related to the problem of excitation transfer between impurity ions in crystals. The way it occurs in CaF_2:Tm^{2+} is unique, since it depends on the magnitude of the hyperfine splittings in the ground and excited states being almost identical. The process appears as a fast relaxation rate which tends to bring the populations associated with the hyperfine splittings in the ground and excited states into thermal equilibrium with one another.

II. OPTICAL AND MICROWAVE PROPERTIES OF CaF_2:Tm^{2+}

The lowest configuration of the divalent thulium ion is a single hole in the $4f$ shell $[4f^{13}]$ with the two spin-orbit multiplets $^2F_{5/2}$ and $^2F_{7/2}$. The splittings of these multiplets in CaF_2 as determined by Kiss[5] are shown in Fig. 1, along with the absorption bands associated with the $4f$-$5d$ transitions from the ground state. The $E_{5/2}$ component of the $^2F_{5/2}$ multiplet is metastable with a lifetime of about 5 ms at 4°K.(5) This level can be populated by pumping into the bands. The radiative decay out of the level via a magnetic-dipole transition to the ground state is narrow enough and occurs with sufficient quantum efficiency that this system has been operated as a cw three-level laser at liquid-helium temperatures.[6]

The ground state splits in a magnetic field with an effective g value of $(+)$ 3.454 and has a hyperfine splitting with the 100% naturally abundant Tm^{179} nucleus $(I=\frac{1}{2})$ of $(-)$ 1101.36 Mc/sec.[7] In the excited state we have measured the effective g value to be $(-)$ 1.453 and the hyperfine splitting to be $(+)$ 1160 Mc/sec.(1)

The energy spacings of these two states in a high magnetic field with the allowed optical transitions are shown in Fig. 2. The notation we use to describe these levels is $[m_s,m_I]$, where $m_s=\pm$ is the effective electron-spin magnetic quantum number (the $\frac{1}{2}$ is usually dropped) followed by $m_I=\pm$ which is the nuclear-spin magnetic quantum number. An asterisk is used to designate the excited state and when absent the ground state is implied. The selection rules for the optical transitions are $\Delta m_I=0$, $\Delta m_s=0(\pi)$ and $\Delta m_I=0$, $\Delta m_s=\pm 1(\sigma)$; the σ transitions have twice the intensity of the π transition.

The strongly allowed EPR transitions are $\Delta m_s=\pm 1$ and $\Delta m_I=0$. At a fixed microwave frequency the transitions for $m_I=-\frac{1}{2}$ occur at a lower magnetic field than those for $m_I=+\frac{1}{2}$. The intensity of the absorption for the low-field line in the ground state using the approximation $h\nu \ll kT$ is

$$S(\mathrm{lf})=C[n(-\,-)-n(+\,-)]$$
$$\cong\tfrac{1}{2}CN\frac{g\beta H(\mathrm{lf})+\frac{1}{2}|A|}{2kT}=\frac{CNh\nu}{4kT}, \qquad (1a)$$

and, for the high-field line,

$$S(\mathrm{hf})=C[n(-\,+)-n(+\,+)]$$
$$\cong\tfrac{1}{2}CN\frac{g\beta H(\mathrm{hf})-\frac{1}{2}|A|}{2kT}=\frac{CNh\nu}{4kT}, \qquad (1b)$$

where C is a constant of proportionality that depends on the details of the microwave circuit and crystal geometry; $n(m_s,m_I)$ is the populations of the sublevels; N is the total number of ions in the ground state; $g\beta H(\mathrm{lf})$ and $g\beta H(\mathrm{hf})$ are the Zeeman splittings for which the high- and low-field lines are in resonance with with the fixed microwave frequency; A is the hyperfine splitting; T is the temperature of the system; ν is the microwave frequency; and k is the Boltzmann constant.

---

[2] D. H. Tanimoto, W. M. Ziniker, and J. O. Kemp, Phys. Rev. Letters **14**, 645 (1965).

[3] G. F. Imbusch and S. Geschwind, Phys. Rev. Letters **17**, 238 (1966).

[4] *Optical Properties of Ions in Crystals*, edited by H. M. Crosswhite and H. W. Moos (John Wiley & Sons, Inc., New York, 1967), p. 171. Kisliuk *et al.*, have recently suggested that similar effects are observed in CaF_2:Eu^{2+} [P. Kisliuk, H. H. Tippins, C. A. Moore, and S. A. Pollack, Phys. Rev. **171**, 336 (1968)].

[5] Z. J. Kiss, Phys. Rev. **127**, 718 (1962).

[6] R. C. Duncan, Jr., and Z. J. Kiss, Applied Phys. Letters **3**, 23 (1963).

[7] W. Hayes and J. W. Twidell, J. Chem. Phys. **35**, 1521 (1961).

With the pump radiation on, the spins in the ground state are heated, so that three temperatures (or parameters) are needed to describe the population distribution between the four sublevels. However, we have the reasonable physical restriction that there is no measurable polarization of the nuclei under the conditions described in this paper, and so two temperatures (or parameters) are sufficient.[8] These are most conveniently taken as the Zeeman and hyperfine temperatures defined by

$$n(m_S,m_I)=\frac{N}{\Gamma}\exp\left\{-\frac{W_Z(m_S,m_I)}{kT_Z}-\frac{W_H(m_S,m_I)}{kT_H}\right\}, \quad (2)$$

where W_Z and W_H are the Zeeman and hyperfine energy eigenvalues, respectively, and Γ is the appropriate normalizing factor that makes the sum of the populations of the sublevels equal to N. When the eigenvalues are small, the temperatures are given approximately by

$$g\beta H/kT_Z\cong 2/N[[n(-\,-)-n(+\,-)] \\ +[n(-+)-n(+\,+)]], \quad (3a)$$

$$|A|/2kT_H\cong 2/N[[(-\,-)-n(+\,-)] \\ -[n(-\,+)-n(+\,+)]]. \quad (3b)$$

The EPR signals are then given by

$$S(\mathrm{lf})=\frac{CN}{4k}\left[\frac{g\beta H(\mathrm{lf})}{T_Z}+\frac{|A|}{2T_H}\right]$$

$$=\frac{CN}{4k}\left[\frac{h\nu}{T_Z}+\tfrac{1}{2}|A|\left(\frac{1}{T_H}-\frac{1}{T_Z}\right)\right], \quad (4a)$$

$$S(\mathrm{hf})=\frac{CN}{4k}\left[\frac{g\beta H(\mathrm{hf})}{T_Z}-\frac{|A|}{2T_H}\right]$$

$$=\frac{CN}{4k}\left[\frac{h\nu}{T_Z}-\tfrac{1}{2}|A|\left(\frac{1}{T_H}-\frac{1}{T_Z}\right)\right]. \quad (4b)$$

Similar expressions can also be defined for the EPR absorption signals in the excited state where all the appropriate terms in Eqs. (3) and (4) are replaced by the corresponding quantities for the excited state, the change in the signs of g and A also being observed.

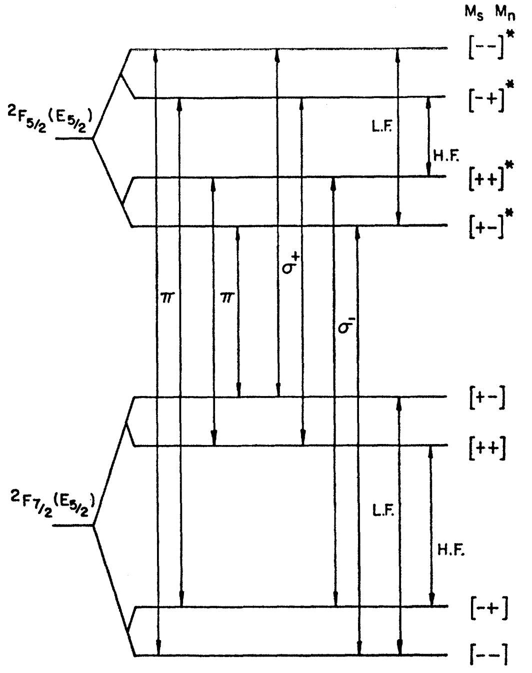

FIG. 2. Allowed optical transitions between the magnetic sublevels of the $E_{5/2}(\frac{5}{2})$ and $E_{5/2}(\frac{7}{2})$ states.

When the optical radiation is present, the ions are continually pumped into the higher electronic states at some rate (P), which is the same for all the ions when the light is incident perpendicular to the magnetic field direction. If the electrons lose all sense of orientation by the time they return to the ground state, then this pumping heats the spins. In a very real sense the spins tend to see the very high temperature associated with the optical radiation. Quantitatively, the rate equations can be solved to show that the steady state of a simple two-level system under these conditions is given by

$$\frac{n(-)-n(+)}{N}=\frac{h\nu}{2kT}\left[\frac{1}{1+P/2R}\right], \quad (5)$$

where P is the rate at which each ion absorbs a photon and R is the relaxation rate of the spins.

All nuclear-spin-flipping processes in the ground state are weak, and, as is demonstrated in a later section of this paper, even the optical pumping cycle does not tend to flip the nuclear spin, so that the expression given in Eq. (5) can be applied separately to the two nuclear-spin states of thulium. Although the electron spin relaxation rates for the two hyperfine components should be almost identical, for the crystals used in these experiments the low-field component was faster by as much as a factor of 3. This is because the dominant mechanism for relaxation was cross relaxation with some other spin system in the crystal. Another feature of this cross relaxation was that the rate changed only by a factor of 2 or 3, for frequencies from 3 to 30 GHz and was typically around 1 sec^{-1} at 1.4°K. For these reasons it is difficult to establish exactly what the ground-state population looks like under conditions of intense optical pumping, but the general feature is that the spins are heated and the net spin orientation is reduced.

---

[8] L. F. Mollenaur, W. B. Grant, and C. D. Jeffries, Phys. Rev. Letters **20**, 488 (1968).

III. MECHANISMS DETERMINING THE POPULATION DISTRIBUTION IN THE EXCITED STATE

A. Thermalization

If each sublevel in the excited state is populated with equal probability and the spins simply relax to the lattice temperature, then the steady-state population differences are given by

$$[n(+\,-)^*-n(-\,-)^*]=\tfrac{1}{2}N^*\frac{|g^*|\beta H+\frac{1}{2}A^*}{2kT^*}\,, \quad (6a)$$

$$[n(+\,+)^*-n(-\,+)^*]=\tfrac{1}{2}N^*\frac{|g^*|\beta H-\frac{1}{2}A^*}{2kT^*}\,, \quad (6b)$$

where $N^*\cong PN/(P+S)$, the total number of ions in the excited state; $1/T^*=[R^*/(S+R^*)][1/T]$, the effective temperature in the excited state; S is the decay rate out of the excited state; and R^* is the spin relaxation rate in the excited state.

The rate at which the spins reach this equilibrium value when disturbed is given by $S+R^*$. Within experimental error, a total rate equal to S is measured. A reasonable guess for R^* would be to take the same relaxation rate as observed in the ground state, 1 $\sec^{-1}$, which, combined with a decay rate of 200 $\sec^{-1}$, makes the effective temperature in the excited state 200 times as hot as the bath. This would make it very difficult, if not impossible, to observe the excited-state EPR resonances if direct thermalization were the dominant mechanism that determined the population distribution in the excited state. However, because of this decoupling from the bath the population distribution can be strongly influenced by other processes which are normally masked by this normal form of spin relaxation.

B. Reabsorption of Fluorescence Radiation

All the crystals used in the experiments were optically dense in the pump bands since every pump photon was needed to obtain a useable EPR signal in the excited state. The peak-absorption cross section for the resonant 1.1-μ fluorescent radiation is roughly the same as that in the $4f$-$5d$ bands ($\approx 10^{-18}$ cm^2), so the crystals are optically dense to this radiation as well. According to Kiss[5] the quantum efficiency for the fluorescence is only 1–2%, so that in a steady-state situation the fluorescent radiation is only 1–2% of the pump radiation present in the crystal. This means that the trapped fluorescence can at best affect the same small percentage of ions in the excited state. The distortion due to reabsorption on the distribution of the radiation which leaves the crystal is very severe and would make any optical studies on the population distributions in the excited state difficult if this transition were used.

It is hard to calculate in detail the effect that reabsorption has on the population in the excited state, because of the question of geometry. For very low optical densities it is clear that there is no effect. If about half the radiation escapes the crystal, then it can be seen from Fig. 2 that the σ radiation and the π radiation tend to oppose one another in their effect on the excited-state Zeeman temperature. Since the σ radiation is twice as probable it would dominate, and so one would expect reabsorption to make T_Z^* slightly positive, the σ^- radiation being more strongly reabsorbed than the σ^+ radiation because of the ground-state thermal distribution.

In an optically dense crystal where most of the radiation is reabsorbed, the effect on the excited-state Zeeman temperature is reduced, since all the photons are equally reabsorbed. However, the hyperfine temperature can be changed under these conditions, since the hyperfine components of the σ transitions are in resonance. Thus, the more heavily populated ground-state $[-\,-]$ level is more likely to absorb a σ^- photon than the $[-\,+]$ level, hence the excited-state $[+\,-]^*$ level is more heavily populated than the $[+\,+]^*$ level. Taking the small quantum efficiency into account, this would lead the inverse of the excited-state hyperfine temperature to be of the order of 1% of the one that is ground state.

C. Optical Cross Relaxation

Closely related to the real process of fluorescence trapping described in Sec. III B is the virtual process of excitation transfer. That is, the excitation of an ion in the metastable level can move rapidly from ion to ion by means of the magnetic dipole-dipole interaction between neighbors (magnetic because the optical transition is a magnetic dipole transition). Since the fluorescence from the metastable level to the ground state in $\mathrm{CaF_2{:}Tm^{2+}}$ is an extremely narrow no-phonon line, this transfer of excitation can take place extremely rapidly in this system. Indeed it may account for the poor quantum efficiency in this transition, since the excitation can rapidly move between $\mathrm{Tm^{2+}}$ ions until it comes to a fluorescence-quenching center; $\mathrm{Tm^{3+}}$, for instance.[9]

Normally, this energy transfer would just move the excitation around and not change the net population distribution among the magnetic sublevels in the excited state, since it is most effective when the energy separations of the neighbors are in exact resonance. But since the hyperfine components of the σ transitions are almost in exact resonance (see Fig. 2) this process can thermalize T_H^* to T_H.

The following calculation can be made to show the effectiveness of this process. The rate of transfer via the dipole-dipole interaction between identical ions which have a sharp no-phonon line to the ground state has been given as[10]

$$R(l)=0.90\times 10^8(\lambda^4 f^2/n^2\Delta\lambda l^6)\ \sec^{-1}\,, \quad (7)$$

---

[9] M. N. Tolstoi and P. P. Feofilov, Opt. i Spektroskopiya 16, 372 (1964) [English transl.: Opt. Spectry. (USSR) 16, 206 (1964)].

[10] D. L. Dexter, J. Chem. Phys. 21, 836 (1953).

where λ is the wavelength of the transition in Å, f is the oscillator strength of the line, $\Delta\lambda$ is the linewidth in Å, l is the spacing between the ions in Å, and n is the index of refraction. For the transition in CaF_2:Tm^{2+}, $\lambda = 1.116p$, $f = 5\times10^{-8}$, and $\Delta\lambda \leq 0.02$ Å.[11] Taking $\Delta\lambda = 0.015$ Å and assuming a uniform index of refraction, Eq. (7) gives for nearest neighbors ($l_0 = 3.86$ Å) a transfer rate of 3×10^7 sec^{-1}, which is much faster than the decay rate of $S \approx 200$ sec^{-1}. A simple rate-equation model can be set up to show that if the ions were separated uniformly by a distance l the hyperfine temperature in the excited state would be given by

$$\frac{1}{T_H{}^*} = \frac{R(l)}{S+R(l)}\frac{1}{T_H}. \tag{8}$$

Since $R(l)$ is such a rapidly decreasing function of l, this expression can be simplified for a dilute doping by saying that all excited ions with a neighbor within a critical distance l_c thermalize completely to T_H, and those which are isolated by a distance greater than l_c do not thermalize at all. The measured hyperfine temperature in the excited state is then given by calculating the percentage of ions which have at least one neighbor within a distance l_c, that is,

$$1/T_H{}^* = 1/T_H[1-\exp(-\tfrac{4}{3}\pi l_c{}^3\tfrac{1}{2}N)], \tag{9}$$

where l_c is defined by

$$R(l_c) = S = 3\times10^7[l_0/l_c]^6 = 200 \text{ sec}^{-1}. \tag{10}$$

$\frac{1}{2}N$ is used for the concentration, since the probability is about $\frac{1}{2}$ that the neighboring will be in one of the ground-state sublevels which will be in resonance with the excited ion. (That is, if the excited ion is in the state $[+,+]^*$ the resonance transfer can take place only if the ground-state ion is in either of the states $[-\,+]$ and $[-\,-]$ and cannot if the ground-state ion is in the states $[+\,+]$ or $[+\,-]$.) When the concentration is given as the percent of thulium ions to calcium sites Eq. (9) becomes

$$1/T_H{}^* = 1/T_H[1-\exp(-6\times10^2N)]. \tag{11}$$

For a 0.05% concentration, this gives $T_H{}^{*-1} = 0.24T_H{}^{-1}$, and $T_H{}^{*-1}$ falls off roughly linearly with concentration. At higher concentrations $T_H{}^{*-1}$ rapidly saturates at $T_H{}^{-1}$ and becomes independent of concentration.

This crude calculation shows that the hyperfine optical cross relaxation is more important, than the first two mechanisms. To anticipate the experimental results, we observe this effect to be quite strong in 0.05% and higher concentrations, it is barely visible in a 0.02% sample, and was not observed at all in a 0.01% sample.

Similar effects would probably occur in ruby, since Cr^{3+} in Al_2O_3 is also very efficient at excitation transfer. To affect the population in the excited state, however, the magnetic field would have to be tilted off the c axis of the crystal to bring the magnetic splitting in the $2\bar{E}$ state in resonance with one of the ground-state magnetic splittings.

D. Spin Orientation Memory

As discussed in Sec. VII, there is no reason why the optical pumping into the $4f$-$5d$ bands followed by the decays into the metastable level should completely destroy the orentation of the ions that exists in the ground state. If there is some memory, then the population differences in the excited state are given by the equations

$$\frac{n(-\,-)^*-n(+\,-)^*}{N^*} = \frac{\alpha[n(-\,-)-n(+\,-)]+\gamma[n(-\,+)-n(+\,+)]}{N} \tag{12a}$$

and

$$\frac{n(-\,+)^*-n(+\,+)^*}{N^*} = \frac{\gamma[n(-\,-)-n(+\,-)]+\alpha[n(-\,+)-n(+\,+)]}{N}, \tag{12b}$$

where α is the fraction of orientation transferred with no nuclear spin flip and γ is that fraction transferred with nuclear spin flip. These equations lead to the effective temperatures

$$T_Z{}^{*-1} = -\tfrac{1}{2}(\alpha+E)|g/g^*|T_Z{}^{-1} = -1.2(\alpha+\gamma)T_Z{}^{-1} \tag{13a}$$

and

$$T_H{}^{*-1} = -\tfrac{1}{2}(\alpha-\gamma)|A/A^*|T_H{}^{-1} = -0.5(\alpha-\gamma)T_H{}^{-1}, \tag{13b}$$

where the negative sign of g^* and A have been taken into account.

There is no way to calculate *a priori* the magnitudes and signs of α and γ, but they should be functions of the wavelength of the pump radiation and in the case of CaF_2:Tm^{2+} it turns out they are also functions of the polarization of the pump radiation. Of all the mechanisms considered so far, this is the only one which can invert $T_Z{}^*$, although it doesn't necessarily have to. What is observed experimentally is a wavelength- and polarization-dependent $T_Z{}^*$ which is also inverted and so fits all these conditions for spin orientation memory.

E. Other Mechanisms

Imbush and Geschwind[3] mention the possibility that the ions might thermalize in some other level above the metastable level in question, and then the decay to the metastable level conserves this new orientation. This process will have the same appearance as the orientation memory from the ground state, except that the

---

[11] Z. J. Kiss and P. N. Yocom, J. Chem. Phys. 41, 1511 (1964).

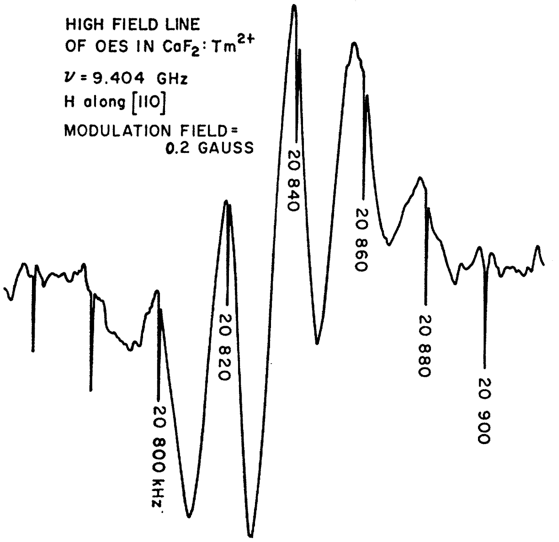

Fig. 3. High-field line of the optically excited state in CaF_2:Tm^{2+}. H along [110] axis, modulation field at 0.2 G.

ground-state temperatures in Eqs. (13a) and (13b) would have to be replaced by the effective temperatures in this other level. This phenomenon could also have a dependence on the pump frequency, but it is hard to imagine how the polarization of the pump radiation could affect it. As Imbush and Geschwind have done in ruby, we also have been able to rule this possibility out by saturating the ground-state resonances, thus changing T_Z and T_H and observing the appropriate changes in the excited state. Although other more exotic processes could be considered, nothing observed in the experiments could not be explained by the first four mechanisms discussed in this section.

IV. EXPERIMENTAL APPARATUS

Most of the measurements described in this paper were made with a standard X-band EPR spectrometer using a superheterodyne system and phase-sensitive detection. The samples were placed against the side wall of a rectangular X-band cavity operating in the TE_{101} mode which contained many slots to allow the optical radiation to enter. A few measurements were also made with an X-band cavity which had provisions for both optical and 0.7-cm^{-1} radiation to enter, which enabled us to do triple-resonance experiments.

The optical source was a 500-W compact dc mercury arc. The radiation from the lamp was collimated with an $f/3$ lens and then focused, in a direction normal to the magnetic field, onto the crystal with a similar lens just outside the Dewar. Provisions were made for introducing filters and optical attenuators in the collimated region of the light beam. The infrared (IR) was always removed with one or more Corning 1-69 filters. Interference filters with a 50 Å bandwidth were used to select the 5461 Å mercury line or the 5770–5790 Å mercury lines. The highest optical power incident on the crystal using these filters was around 100 mW.

The experiments were all performed with the crystal in pumped liquid helium at roughly 1.4°K, although the resonances have been observed at 4.2°K. The Dewar was of a standard glass variety with the area about the cavity not silvered. The pump radiation passed through the liquid nitrogen and liquid helium. The cavity and sample were always immersed in the superfluid helium to keep the temperature changes small while optically pumping. The temperature never changed more than 0.1–0.2°K under short (<1 min) intense applications to the light.

To obtain maximum signal-to-noise, a field modulation of about 7 G was generally used which is equal to half the EPR linewidth. To illustrate the sensitivity of our detection system, Fig. 3 shows a standard derivative resonance curve of the high-field line in the optically excited state (OES) taken with a 0.2-G modulation field and the dc field oriented along the [110] axis. The in-

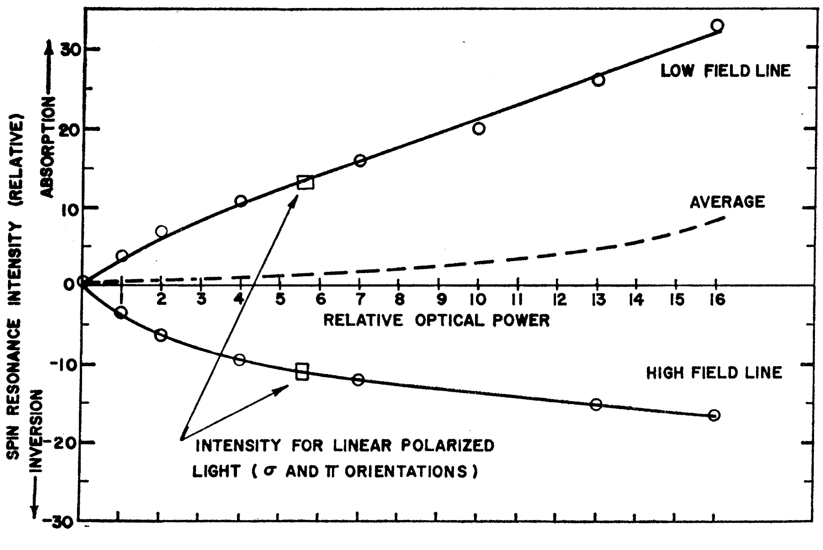

Fig. 4. Intensity of the two EPR lines in the OES in 0.05% CaF_2:Tm^{2+} as a function of pump in power at 5460 Å.

tegration time was 0.2 sec and the complete sweep took about 3 min. This figure shows the superhyperfine structure associated with the interaction with the neighboring eight fluorines, curiously it disappears along the [001] direction and is not as distinct along the [111] direction. The superhyperfine results have not been analyzed.

The calcium fluoride crystals used were grown doped with TmF_3 by both RCA and Optovac and we reduced most of the thulium to the divalent state by heating the crystals in a calcium atmosphere.[11] Measurements were made on 0.01- to 1.0-mole% concentrations of thulium. The crystal sizes used were usually about 6×6 mm and 1-mm thick and oriented so that the normal to the large face of the crystal was parallel to the pump radiation and perpendicular to the magnetic field. For all the crystals the shortest distance was optically dense (optical density of 1 or greater) so that most of the pump photons were absorbed in the crystal.

V. EXPERIMENTAL RESULTS

A. Pumping with 5460 Å Radiation

Figure 4 shows the peak intensity of the two excited-state EPR lines for a 0.05% sample as a function of the incident pump power, while pumping only with the mercury green line. The striking feature is that the intensities of the two hyperfine components are about equal in magnitude and opposite in sign, the high-field line being inverted. The population energy-level diagram in Fig. 5(a) graphically shows what these results imply, and referring to Eqs. (4a) and (4b), it is apparent that the temperature parameter T_Z^{*-1} is zero. These conditions are explained by the optical cross-relaxation process described in Sec. IV C.

The intensities of the two lines start out linear in the effective pump rate P, then as this rate becomes comparable to the ground-state spin relaxation rate R, the temperatures in the ground state become high and this saturates the signal in the excited state.

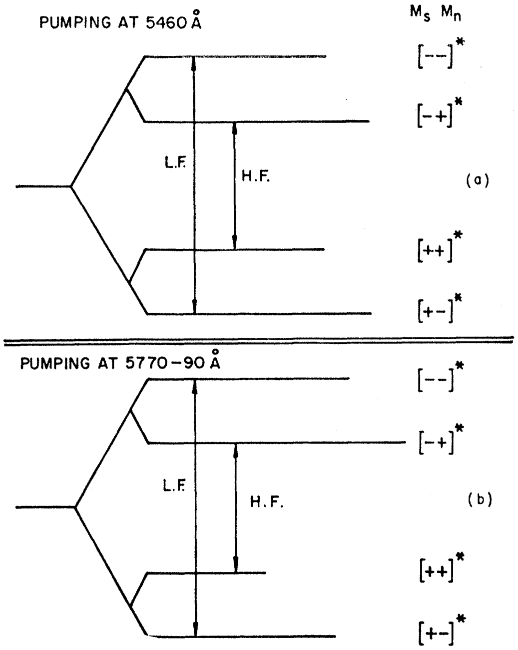

FIG. 5. Population distribution in OES in the 0.05% CaF_2:Tm^{2+} crystal pumping with (a) 5460 Å radiation and (b) 5770–90 Å radiation, the length of the horizontal lines being proportional to the populations.

B. Pumping with 5770–90 Å Radiation

Figures 6 and 7 show the peak intensities of the two excited-state EPR lines in the same 0.05% sample and a 0.02% sample as a function of the incident pump power while using the yellow mercury lines. The power available in the yellow is slightly higher than that in the green, and we have observed that the net heating of the

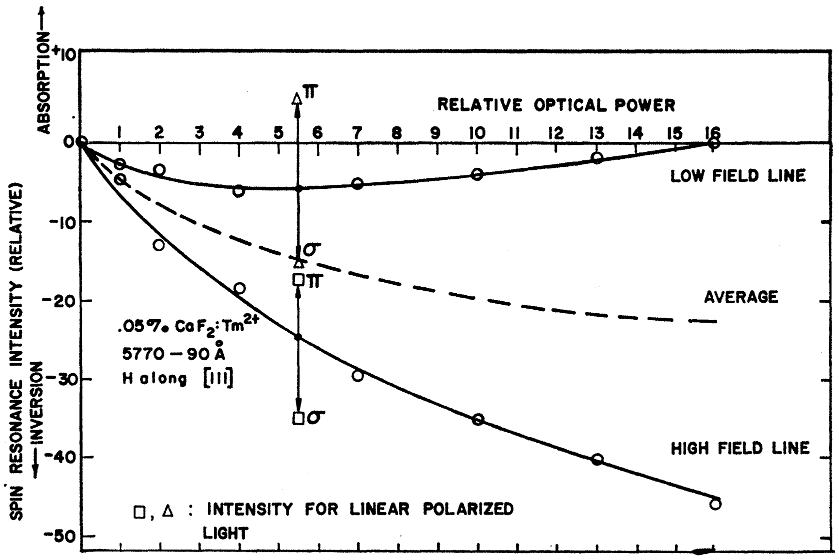

FIG. 6. Intensity of the two EPR lines in the 0.05% CaF_2:Tm^{2+} crystal as a function of pump power at 5770–5790 Å.

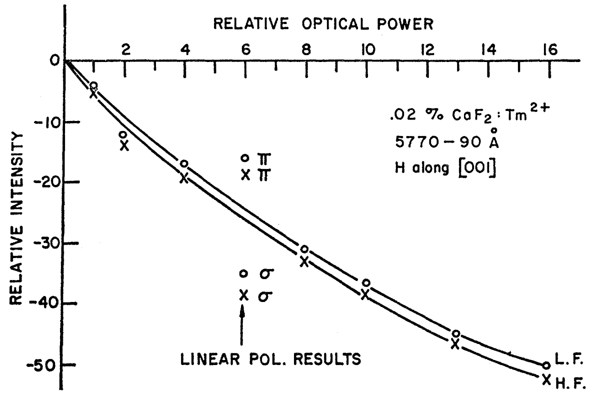

FIG. 7. Intensity of the two EPR lines in the 0.02% CaF_2:Tm^{2+} crystal as a function of pump power at 5770–5790 Å.

ground-state spins is about the same for both lines, so the horizontal scales in Figs. 4 and 6 are approximately the same for the 0.05% sample. The important feature in Fig. 6 is that the average intensity of both lines is emissive, $T_Z^{*-1}<0$. This implies that another effect is superimposed on the optical cross-relaxation process which we claim is spin orientation memory.

Confirmation of this interpretation is shown by the introduction of the linear polarizer into the pump beam. The intensities of the excited-state EPR lines are shown in Figs. 4 and 6 when the polarizer is in the π (the electric vector parallel to the magnetic field) and σ (the electric vector perpendicular to the magnetic field) orientations. No change is observed for pumping with the green where there is no spin orientation memory, while large changes are seen for the yellow radiation.

The two effects on the excited state are additive, since only a small number of ions is affected by both mechanisms. Since the data taken with green radiation reflect only optical cross relaxation, the intensities in Fig. 4 can be subtracted from the corresponding values in Fig. 6 for the 0.05% sample and the resultant curves for the high- and low-field lines will be almost identical and reflect only orientation memory. Conversely, the data in Fig. 7 for the 0.02% sample show that the two components have almost the same intensity, implying little effect from optical cross relaxation, so it should be, and is, extremely difficult to see the resonances in this sample when the green pump radiation is used.

C. Pumping with $\lambda \geq 5400$ Å Radiation

Figure 8 shows the results for pumping the 0.05% sample with the radiation from the mercury lamp filtered to wavelengths longer than 5400 Å with a Corning 3-71 sharp-cut filter, (the IR filters also being present). The power available is slightly less than 10 times that with the yellow or green lines alone, so that the ground-state spins can be driven past the point where $P=R$. The intense pumping heats up the Zeeman and hyperfine temperatures in the ground state, which decreases the effectiveness of both orientation memory and the hyperfine optical cross relaxation. The latter effect is shown by the saturation in the difference between the intensities of the two EPR lines. The destruction of orientation in the ground state is demonstrated by the average intensity of the two lines becoming absorptive at the high pump levels. The final absorptive signal for both components comes from direct thermalization in the optically excited state.

When this pump radiation is suddenly turned on at a high level, both EPR lines in the excited state are initially emissive and then decay quickly to the steady-state values shown in Fig. 8. This behavior reflects in a dynamic way the destruction of the orientation in the ground state. This rate of decay in the excited state was measured to be 2.9 sec^{-1} at the maximum pump level. When the magnetic field was lowered from 4.5 to 2 kG so that the effect on the ground-state EPR resonance could be observed, the same pump level destroyed the ground-state magnetization at the rate of 2.4 sec^{-1}. The rate at which these decays occur is the sum of the effective pump rate P and the spin relaxation rate of the ground-state spins R. The difference between the measured rates of 2.9 and 2.4 sec^{-1} is then explained by the change in R for the two field values, which were measured in this crystal at 1.4°K to be 1.2 sec^{-1} at 4.5 kG, and 0.83 sec^{-1} at 2.0 kG, respectively. This gives then a dynamic confirmation to the transfer of orientation.

D. Concentration Dependence

The hyperfine optical cross-relaxation process should be concentration-dependent as discussed in Sec. IV C, while the transfer of orientation should be independent of concentration. Direct thermalization can be concentration-dependent if the relaxation rate in the excited state is. In the preceding results for the 0.02% and 0.05% samples, it is clear that the optical cross relaxation and orientation memory change as expected. In a 0.01% sample we could only observe the resonance with yellow pumping, and both hyperfine components had the same intensity. A few measurements were also made on 0.2% and 1.0% samples. In these samples the optical cross relaxation was quite strong (i.e., the low-field line was always the more absorptive component) and also the direct thermalization became important. In the 1.0% sample under all conditions both excited-state resonances were always absorptive.

E. Triple Resonance

An X-band ($\sim$0.3 cm^{-1}) cavity was constructed with openings for optical and K-band ($\sim$0.7 cm^{-1}) radiation to enter. Using this structure we could optically pump a crystal and monitor the OES resonances while simultaneously saturating one of the ground-state resonances with K-band radiation. The X-band frequency was fixed by the loaded cavity frequency and so each combination of OES resonance observed and ground-state resonance saturated required a different K-band frequency. The power level of the K-band radiation in the cavity could not be made identical for each frequency, and so the degree of saturation of the ground-state levels was not the same. In addition, when one of the resonant lines in the ground state is saturated we are not absolutely sure what the net effect is on the whole ground-state population, although there is evidence that the states of opposite nuclear-spin orientation seem to be fairly independent of one another. One further difficulty is the effect of the optical pump on the ground-state population distribution is not negligible as the appearance of saturation in the pump-power curves in Figs. 3, 5, and 7 show. The result of all these uncertainties in such a complicated situation allows only qualitative conclusions be drawn from the experiments.

If we assume that the optical pumping does not change the ground-state spin population and also assume that the states of opposite nuclear-spin orientation are independent, the effects of saturating one of the ground-state EPR lines can be calculated. Referring to Eq. (2), which defines the hyperfine and Zeeman temperatures, it can be shown that when the high-field or low-field line in the ground state is completely saturated the effective temperatures become

$$T_Z^{-1} \cong \tfrac{1}{2} T^{-1} \tag{15a}$$

and

$$T_H^{-1} = \pm(\nu/A) T^{-1}, \tag{15b}$$

the plus sign in the hyperfine temperature being used when the high-field line is saturated and the negative when the low-field line is saturated. Since the K-band frequencies used were about 20 GHz and the hyperfine constant is about 1 GHz the effect on the hyperfine temperature is to make it extremely small in magnitude. This can be seen in Fig. 9, which graphically shows the effects of saturation. Inclusion of the effects of the optical pump and nuclear-spin-flip relaxation processes will tend to reduce such a large change in T_H but it will always be larger than any change in T_Z. This makes observations of the effects of saturating the ground-state EPR lines on the hyperfine optical cross relaxation process in the excited state very easy, but obscures the effects on the transfer of spin orientation.

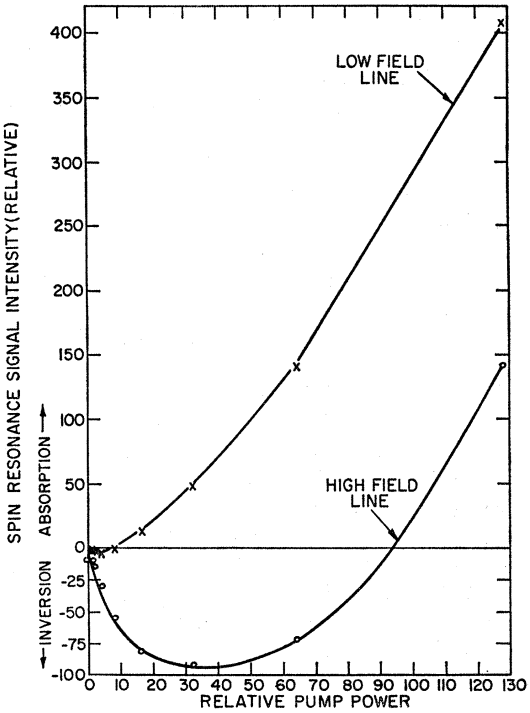

FIG. 8. Intensity of the two EPR lines in the 0.05% CaF$_2$:Tm^{2+} crystal as a function of pump power for $\lambda \geq 5400$ Å.

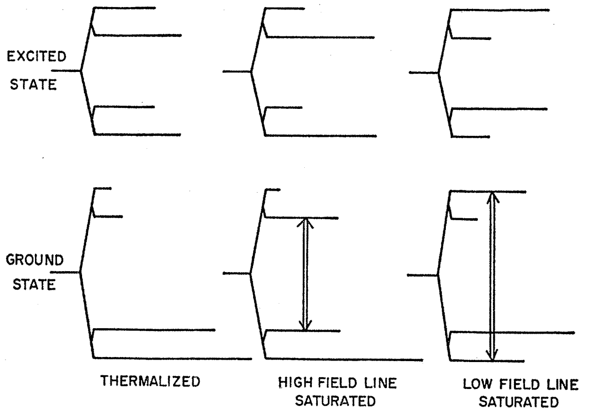

FIG. 9. The effect of saturation of the ground-state resonances on the OES population when only the optical cross-relaxation mechanism is operative.

When the excited state is populated by pumping with the green mercury line there is little or no transfer of magnetization and so $T_Z^* \cong 0$. The strength of the high- and low-field EPR lines in the excited state are then proportional to $\pm T_H^{-1}$, respectively. When the ground-state high-field line is saturated the two excited-state EPR lines should become much stronger but keep the same signs, and when the ground-state low-field line is saturated the excited-state EPR lines should also be intense but flipped over. We show the expected OES populations graphically in Fig. 9, which makes it easier to visualize the situation. Table I gives the experimental results for the 0.02% sample where this is confirmed. The change is dramatic in this low-concentration sample, since without the saturating K-band radiation, the OES resonances can hardly be observed while pumping with the maximum power available in the green.

When the OES is populated by pumping with the yellow mercury radiation then transfer of spin orientation from the ground state is present in addition to optical cross relaxation. The experimental results under identical K-band saturation conditions as those pumping with the green are also shown in Table I. Even though the optical cross relaxation is weak at this low concentration, for the reasons outlined above it strongly affects the results. The best way we have found to dis

TABLE I. The intensity of the two OES resonances in 0.02% $CaF_2:Tm^{2+}$ for various conditions of pump wavelength excitation and ground-state saturation.

Wavelength of excitation	5460 Å		5770–5790 Å	
Excited-state line	High field	Low field	High field	Low field
Ground state				
No saturation	∼0	7	−58	−44
High-field line saturated	−48	46	−68	−8
Low-field line saturated	63	−24	15	−44

play the effect of saturation of the ground-state resonances on the spin orientation memory is simply to subtract the values for pumping with 5460 Å radiation from the corresponding values for pumping with 5770–90 Å radiation, the results of which are given in Table II. The rationale behind this is first that the amounts of power available in the green and yellow lines in our lamp are almost identical, and the measured effect on the ground state is found to be the same for these two pump conditions. Secondly, the effects of both mechanisms on the whole population in the excited state are small, and so they act independently and are additive. Thirdly, the optical cross relaxation is independent of pump frequency, and so the results of pumping with the green, which directly reflect its effects, should be simply superimposed on the transfer of magnetization effects when we pump with the yellow. This procedure has the added advantage that it does not require a detailed understanding of the degree of saturation achieved nor the various other uncertainties involved in the effects on the ground-state population, since the ground-state population distributions should be roughly the same under these nearly identical conditions.

The results in Table II show the interesting feature that when the ground-state levels which have the same nuclear-spin orientation as monitored in the OES are saturated the effect decreases the intensity of the emissive signal by about a factor of 3, while if they are of opposite nuclear-spin orientation the effect is much smaller. This shows that we have very strong nuclear-spin orientation memory during the optical pumping, at least for those ions which have retained some electron-spin orientation memory during the optical pump cycle.

TABLE II. The difference between the intensities for 5770–90 and 5460 Å excitation as given in Table I.

	Difference between 5770–5790 and 5460 Å results	
Excited-state line	High field	Low field
Ground state No saturation	−58	−51
High-field line	−20	−54
Low-field line	−48	−20

That the transfer of orientation takes place with a high degree of nuclear-spin memory is further confirmed by the effect that saturation has on the influence of pump polarization on the OES population distribution. Table III shows the OES resonance intensities for σ and π polarization pumping with the various ground-state resonances saturated for excitation with both green and yellow radiation. The interesting feature in the results of pumping with the yellow is that all differences between σ and π polarizations disappear only when the resonances in the ground and excited states for the same nuclear-spin orientation are used.

Again, the direct subtraction of the green from the yellow results show the effects of spin memory more clearly. This is given in Table IV. Note that not only does the polarization dependence disappear under saturation, but also the absolute magnitude of the signal is decreased when the same nuclear-spin orientation is involved. The results in this table indicate almost complete nuclear-spin orientation memory for those ions involved in the transfer of spin orientation.

F. Dependence on Polarization and Wavelength of Pump Radiation

When pumping at 5790 Å the spin orientation memory is generally about twice as large when pumping with σ polarized light as when pumping with π polarized light. This was investigated carefully in an oriented sample and found to be true whether the magnetic field was along the [001] direction or the [111] direction. This is a curious and important observation, as it should reveal something about the mechanism of the orientation conserving decay into the metastable level, and is discussed in Sec. VII. The effect of pumping with circularly polarized light along the field direction was also investigated, but the results are complicated by the fact that such pumping can change the spin orientation in the ground state.[12] Large differences were indeed observed in the strengths of the resonances in the excited state between right and left circular polarizations, but the sign of the spin orientation could never be reversed.

Crude wavelength-dependence measurements were made by using broad-band filters. No spin orientation memory occurs for wavelengths much longer than 5800 Å, while it appears that around 4000 Å there may be a small amount that has the same sign as observed at 5790 Å. Thus there is no consistant pattern of a monotonically decreasing effect as the pump wavelength gets shorter, which might be expected since more nonradiative decays are needed to reach the metastable level.

---

[12] E. S. Sabisky and C. H. Anderson, J. Quantum Electron. QE-3, 287 (1967).

VII. DISCUSSION OF TRANSFER OF SPIN ORIENTATION

A. General

In this section we would like to present a simple model for the transfer of spin orientation, to indicate how it comes about on general principles and why it is found in such diverse systems as CaF_2:Tm^{2+}, ruby, and the defect center in CaO. In this model the ion is pictured as being excited into a particular state in the bands by the absorption of a photon and then decaying down a ladder of levels by the emission of phonons and possibly photons, one at a time or in coherent multiple sets, until it reaches the metastable level. These discrete steps that the ion makes down from the band are assumed to be entirely due to spontaneous processes. The decays then conserve time-reversal symmetry to the extent that the energy steps taken are large compared to the magnetic splittings induced by the magnetic field. If the pump radiation is incident perpendicular to the magnetic field, polarized, or unpolarized, then the transitions it induces are also symmetrical under time-reversal symmetry. Thus under these conditions the net process of pumping into the metastable level also conserves time-reversal symmetry.

For example, consider the situation where the ground-state and metastable levels are both simple Kramers doublets, e.g., CaF_2:Tm^{2+} without nuclear spin. The restraint of time-reversal symmetry puts the following conditions on the net pump rates from the ground-magnetic sublevels to the excited-state sublevels:

$$P_{1/2\to1/2}=P_{-1/2\to-1/2}$$

and (16)

$$P_{1/2\to-1/2}=P_{-1/2\to1/2}\,.$$

That is, the net spin-flipping rates are the same and the net non-spin-flipping rates are the same, but nothing says that these two should be the same, so in general $P_{1/2\to1/2}\neq P_{1/2\to-1/2}$.

However, if there are a large number of spin-flipping decays involved then the net rates from the ground-state to the metastable level will tend to approach one another. One way to see this is to consider a two-step process to the metastable level. Let P and P' be the non-spin-flip and spin-flip pump rates, respectively, for going from the ground state to the first level and, correspondingly, let R and R' be the decay rates down to the metastable level. Then the net non-spin-flipping pump rate is given by

$$S=(PR+P'R')/(P+R+P'+R')\,, \tag{17}$$

and the spin-flipping rate is given by

$$S'=(PR'+P'R)/(P+R+P'+R')\,. \tag{18}$$

The fractional difference between these rates is given by

$$\frac{S-S'}{S+S'}=\frac{P-P'}{P+P}\cdot\frac{R-R'}{R+R'}\,. \tag{19}$$

TABLE III. The intensity of the two OES resonances in 0.02% CaF_2:Tm^{2+} for various conditions of pump wavelength excitation, polarization and ground-state saturation.

Excitation wavelength	5770–5790 Å				5460 Å			
Excited-state line	High field		Low field		High field		Low field	
Polarization	σ	π	σ	π	σ	π	σ	π
Ground state No saturation	−30	−16	−32	−22	∼0	∼0	∼0	∼0
High-field line	−22	−22	0	8	−19	−19	35	35
Low-field line	− 9	3	−20	−20	20	20	−13	−13

For n-decay steps it is immediately clear that

$$\frac{S-S'}{S+S'}=\frac{P-P'}{P+P'}\prod_{i=1}^{n}\frac{R_i-R_i'}{R_i+R_i'}\,. \tag{20}$$

Except for decays which leave the spins alone or flip all the spins, the magnitude of each multiplier is less than one, and so in the limit of a large number of decays the net fractional difference approaches zero. *If for any step the fractional difference is zero, the net pump difference is zero and all spin orientation memory is destroyed.* Note that by linearly polarizing the pump radiation the relative values of P and P' can be changed, showing how changing the linear polarization can affect the net pump rates.

The above model calculation uses a system that consisted only of isolated Kramers doublets; however, most of the features presented are general in nature. For example, the ground state of the defect center in CaO studied by Kemp[2] is the singlet component of a pair of interacting spin-$\frac{1}{2}$ systems and the metastable level, 200 cm^{-1} above the ground state, is the triplet component. Time-reversal symmetry requires that the two net spin-flip pump rates ($\Delta m_s=\pm1$) have to be equivalent but not necessarily the same as the non-spin-flip pump rate. The experiments clearly show that the latter is larger than the spin-flipping rates. Since both the ground state and the metastable state are never polarized, $\langle S_Z\rangle=0$, this situation really corresponds to a transfer of alignment into the metastable level, but otherwise the features are the same as a transfer of spin orientation.

TABLE IV. The difference between the intensities for 5770–90 and 5460 Å excitation as given in Table III.

	Difference between 5770–5790 and 5460 Å results			
Excited-state line	High field		Low field	
Polarization	σ	π	σ	π
Ground-state line No saturation	−30	−16	−32	−22
High-field line	− 3	− 3	−35	−27
Low-field line	−29	−17	− 7	− 7

B. Application of this Model to $CaF_2:Tm^{2+}$

Using the above model, some conclusions can be drawn about the character of the electronic state in the band that is excited initially when pumping in $CaF_2:Tm^{2+}$ with yellow (5770–90 Å) radiation. Magnetic circular dichroism measurements on these $4f$-$5d$ bands have indicated that the transitions can be described as purely electronic and governed by the selection rules for the electric-dipole operator in the cubic point group.[13] An examination of the coupling coefficients for the electric-dipole operator, when the magnetic field is along the [001] axis, shows that transitions from an $E_{5/2}$ level to levels with $E_{1/2}$ symmetry are forbidden and if equal amounts of σ and π radiation are present (unpolarized light incident perpendicular to the magnetic field) then the spin-flip and non-spin-flip pump rates to an $E_{5/2}$ level are the same, which destroys all information about the magnetization of the ground state [$P=P'$ in Eq. (20)]. Therefore, since we observe orientation memory under these conditions, the state initially populated in the band has to have $G_{3/2}$ symmetry. The magnetic circular dichroism measurements indicate that the $4f$-$5d$ absorption bands at both 5770–90 and 5461 Å are primarily $G_{3/2}$ in character.

It is interesting to carry out the calculation for spin orientation memory for excitation into a $G_{3/2}$ level from the ground-state $E_{5/2}$ level, which is then followed immediately by a single decay into the metastable $E_{5/2}$ level. Assume the decay to take place before any thermalization can take place between the sublevels of the $G_{3/2}$ state. With the magnetic field along the [001] direction and the pump radiation unpolarized and directed perpendicular to the magnetic field, spin orientation memory will occur with the same sign as observed (i.e., the spins keep the same orientation) only if the decay has T_1 symmetry. Also, for this symmetry if the pump radiation is linearly polarized the spin orientation memory should be twice as large for pumping with σ light as with π light, which is close to what we observe. This is interesting because T_1 is the symmetry of the electric-dipole operator, and so this would imply that the decay could be a radiative one. However, the selection rules for optical excitation between an $E_{5/2}$ state and a $G_{3/2}$ state are strongly dependent on the direction of the magnetic field, and for the field along the [111] direction the sensitivity of the memory to the polarization of the pump radiation should be greatly reduced. But we observe about the same magnitude for all orientations of the field. It may be possible to account for this latter point by allowing for a Jahn-Teller splitting of the quartet, but then the model becomes more complicated.

VIII. CONCLUSION

We have shown that spin orientation memory can take place when optically pumping divalent thulium in calcium fluoride into its metastable level. This memory is dependent on the wavelength and polarization of the pump radiation. It also occurs with a high degree of nuclear-spin orientation memory. Although spin orientation memory can be shown to be consistent with the general principle of time-reversal symmetry, the details of the phenomenon are not understood in $CaF_2:Tm^{2+}$. Indeed, it would be useful to explore the pump wavelength and polarization dependence more fully.

We have also shown that there is a rather rapid optical cross relaxation or excitation transfer which takes place between neighboring thulium ions. Because the hyperfine interaction constant is almost the same in the ground and excited states, this excitation transfer plays an important role in determining the population distribution among the sublevels of the metastable state.

ACKNOWLEDGMENT

We wish to acknowledge the assistance of J. Beherrell in carrying out these experiments.

---

[13] C. H. Anderson, H. A. Weakliem, and E. S. Sabisky, Phys. Rev. **143**, 223 (1966).